

Functional Heterogeneity of Endothelial Cells Derived from Human Pluripotent Stem Cells

Saritha S. D'Souza,^{1,*} Akhilesh Kumar,^{1,*} and Igor I. Slukvin^{1–3}

Specification of endothelial cells (ECs) into arterial, venous, and lymphatic cells is a crucial process of vascular development, and expanding our knowledge about EC specification from human pluripotent stem cells (hPSCs) will aid the design of optimal strategies for producing desired types of ECs for therapies. In our prior studies, we revealed that hPSC-derived VE-cadherin(V)⁺CD31⁺CD34⁺ ECs are heterogeneous and include at least three major subsets with distinct hemogenic properties: V⁺CD43/235a⁻CD73⁻ hemogenic endothelial progenitors (HEPs), V⁺CD43^{lo}CD235a⁺73⁻ angiogenic hematopoietic progenitors (AHPs), and V⁺CD43/235a⁻73⁺ non-HEPs. In this study, using angiogenesis assays, we demonstrated that ECs within these subsets have distinct endothelial colony- and tube-forming properties, proliferative and migratory properties, and endothelial nitric oxide synthase and inflammatory cytokine production potentials. Culture of isolated subsets in arterial, venous, and lymphatic conditions revealed that AHPs are skewed toward lymphatic, HEPs toward arterial, and non-HEPs toward venous differentiation in vitro. These findings suggest that selection and enhancement of production of a particular EC subset may aid in generating desirable EC populations with arterial, venous, or lymphatic properties from hPSCs.

Keywords: endothelial cells, human pluripotent stem cells, hemogenic endothelium, heterogeneity

Introduction

ENDOTHELIAL CELLS (ECs) lining different vessels differ in morphology, function, and gene expression. Vascular endothelium consists of a dynamic and highly heterogeneous population of cells that differ not only between various organ beds but also exhibit functional and morphological differences within the same vascular compartment [1–3]. In vivo, ECs perform important barrier functions by forming tight continuous monolayers in organs as in the brain or discontinuous layers in organs such as the kidney and bone marrow, which require rapid exchange of fluids and cells [4,5]. EC diversity is also reflected at the molecular level by vessel size-specific, tissue-specific, and even disease-specific differences [5–12].

During development, ECs emerge de novo from the mesoderm to form a primary vascular plexus. Establishment of arteriovenous fate during development is genetically determined, while blood flow is required for maintaining vascular fate [13,14]. Specialization of the endothelium to arterial, venous, hemogenic, and lymphatic subtypes is necessary to fulfill diverse functions of the vasculature [15,16]. Human pluripotent stem cells (hPSCs) offer the opportunity to study

endothelial development in a dish and produce ECs for therapies. Although multiple protocols for EC generation from PSCs have been established, little is known about EC heterogeneity in hPSC cultures and their specification toward arterial, venous, or lymphatic cells.

In our prior studies, we revealed that VE-cadherin(V)⁺CD31⁺CD34⁺ ECs are heterogeneous and include three major subsets with distinct hematogenic properties: (i) V⁺CD43/CD235a⁻73⁺ nonhemogenic endothelial progenitors (non-HEPs) that have all of the functional and molecular features of ECs, but do not produce blood cells; (ii) V⁺CD43^{lo}CD235a⁺73⁻ angiogenic hematopoietic progenitors (AHPs) that possess primary hematopoietic characteristics and FGF2 and hematopoietic cytokine-dependent colony-forming potential in serum-free semisolid medium, but are capable of generating ECs, and (iii) V⁺CD43/CD235a⁻CD73⁻ hemogenic endothelial progenitors (HEPs) that have primary endothelial characteristics and lack hematopoietic CFC potential and surface markers, but are capable of generating blood and ECs upon coculture with stromal cells or on a matrix with hematopoietic cytokines [17].

In the present study, we assessed the endothelial progenitor potential of these three subsets in vitro and in vivo and their

¹Wisconsin National Primate Research Center, University of Wisconsin, Madison, Wisconsin.

²Department of Cell and Regenerative Biology, School of Medicine and Public Health, University of Wisconsin, Madison, Wisconsin.

³Department of Pathology and Laboratory Medicine, University of Wisconsin Medical School, Madison, Wisconsin.

*These authors contributed equally to this work.

capacity to support arterial, venous, or lymphatic properties following culture in corresponding conditions *in vitro*. We found that AHPs are skewed toward lymphatic, HEPs toward arterial, and non-HEPs toward venous differentiation.

Materials and Methods

Maintenance and differentiation of human embryonic stem cells

The hESC H1 and H9-EGFP human embryonic stem cell (hESC) lines and fibroblast-derived iPSC line DF-19-9-7T were obtained from WiCell Research Institute. The mouse OP9 bone marrow stromal cell line was provided by Toru Nakano (Osaka University, Japan). hPSCs were maintained on irradiated mouse embryonic fibroblasts, as described previously [18], and induced to differentiate in coculture with OP9 stromal cells [19].

Cell sorting and culturing of endothelial subsets

V⁺ cells were isolated from day 5 hESC/OP9 cocultures by positive MACS selection using the corresponding FITC-conjugated antibodies and anti-FITC magnetic beads (Miltenyi). MACS-enriched cells were stained with CD73-PE and CD43 and CD235a-APC antibodies and sorted using an FACS Aria II cell sorter (BD Biosciences) to select EC subsets. Sorted endothelial subsets were cultured on fibronectin (5 µg/mL)-coated plates in TGFβ inhibitor (SB431542; 10 µM) containing the endothelial cell medium (ECM; Sciencell Technology). Media were refreshed every alternate day and cells were passaged at day 4/5.

Single-cell assay

For single-cell assay, FACS was used to place one single live EC/well of a 96-well, flat-bottom tissue culture plate precoated with human fibronectin (5 µg/mL) containing 200 µL of ECM with SB (10 µM) and rock inhibitor. Individual wells were examined under a fluorescence microscope at 20× magnification to ensure that only one cell had been placed into each well. Cells were cultured at 37°C, 5% CO₂, in a humidified incubator. Media was changed every 4 days with fresh complete endothelial media. At day 14, each well was examined for EC growth using VE-cadherin immunostaining and those wells in which two or more ECs were identified under a fluorescence microscope at 20× magnification were scored as positive. To enumerate the number of cells per well, we counted cells by visual inspection with a fluorescence microscope at 20× magnification [20].

In vivo Matrigel model

Animal protocol was approved by the School of Medicine and Public Health Institutional Animal Care and Use Committee at the University of Wisconsin, Madison. Endothelial subset spheroids (1,000 cells per spheroid) were generated as previously described [21]. Cells were suspended in culture medium containing 0.25% (w/v) methylcellulose and seeded on plastic dishes in a hanging drop to allow overnight spheroid aggregation. All suspended cells contribute to the formation of a single spheroid per drop of defined size and cell number. The spheroids gen-

erated from 1×10^6 cells from each subset were harvested and suspended in cold growth factor-reduced Matrigel (BD Biosciences) and fibrinogen (2 mg/mL; CalBiochem) containing 250 ng/mL vascular endothelial growth factor (VEGF) and 250 ng/mL fibroblast growth factor (FGF). For the *in vivo* Matrigel plug assay, 10-week-old NOD-SCID mice were injected subcutaneously in the back with 0.5 mL of Matrigel containing the cells after addition of thrombin (0.4 U; CalBiochem) [22]. Seven days after injection, Matrigel plugs were removed and processed for paraffin embedding. Sections were rehydrated, followed by antigen retrieval using citrate buffer. The sections were stained with mouse anti-human CD31 (Thermo Scientific), mouse anti-human CD43 (Santa Cruz Biotechnology), and mouse anti-human CD45 (E-Biosciences) antibodies. The sections were developed using the HRP/DAB (ABC) IHC detection kit (Abcam). For sections stained with CD45, a green substrate (Biocare Medical) was used. Slides were then counterstained with hematoxylin, dehydrated, cleared, and mounted. The number of total blood vessels and CD43- and CD45-positive cell clusters were manually counted using a Nikon Microphot SA microscope.

Analysis of arterial, venous, and lymphatic endothelial potential

For arterial specification, the FACS-isolated EC subsets were cultured on plates coated with fibronectin (5 µg/mL) and Jagged-1/Fc chimera (1 µg/mL) in endothelial medium (Science Cell Technology) containing 100 ng/mL VEGFA and 0.5 mM 8-Br-cAMP [23]. For venous specification, EC subsets were cultured on fibronectin-coated plates in endothelial medium containing 10 ng/mL VEGFA and 1 µM of γ-secretase inhibitor [24]. For lymphatic specification, EC subsets were cultured on fibronectin-coated plates in endothelial medium and OP9-conditioned medium containing 100 ng/mL VEGFC and 100 ng/mL Ang-1 [25]. Cells were incubated at 37°C and 5% CO₂ for 14 days before harvesting for immunostaining and RNA isolation.

Immunofluorescent staining

For immunofluorescent staining, samples were fixed with 4% paraformaldehyde at 20°C and permeabilized with 0.1% Triton X-100. Blocking solution consisted of PBS, 1% bovine serum albumin, and 5% goat serum. Primary antibodies were diluted in blocking solution and applied overnight at 4°C. The primary antibodies used were VE-cadherin (BD Biosciences), NOTCH1 (Cell Signaling Technology), COUP-TFII (Perseus Proteomics), PROX1 (ReliaTech GmbH), and endothelial nitric oxide synthase (eNOS; BD Biosciences). After incubation, nonspecific binding was washed with a solution of PBS and 0.1% Tween 20. Secondary antibody at a dilution of 1:1,000 in PBS was applied for 1 h at RT. Nonadherent antibody was washed with PBS and 0.1% Tween 20, after which samples were mounted using DAPI (Vector Laboratories) as a nuclear marker. For controls, cells were labeled with unspecific immunoglobulins (Santa Cruz Biotechnology), followed by incubation with the secondary antibody. The immunolabeled cells were examined using the Nikon Eclipse Ti-E confocal system (Nikon Instruments, Inc.).

Tube formation assay

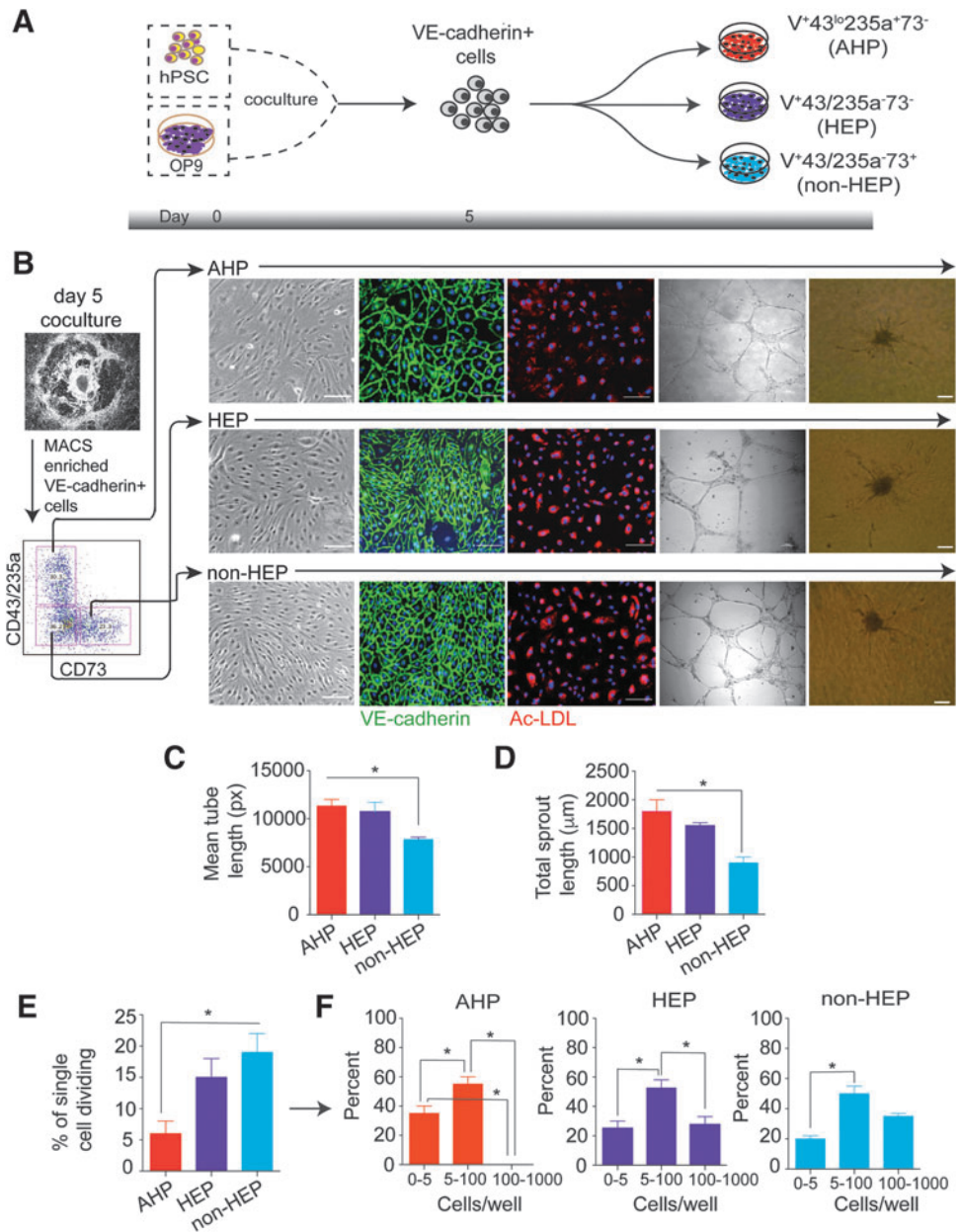
For tube formation assay, endothelial subsets (3×10^4 /well of a 24-well plate) were seeded on presolidified Matrigel™ (BD Bioscience) in EGM-2 media (PromoCell) containing 20 ng/mL VEGF. The cells were incubated for 24 h at 37°C, 5% CO₂, in a humidified atmosphere. The vascular network was photographed at indicated time points using a Nikon Eclipse Ti-E configured with an AIR confocal system (Nikon Instruments, Inc.) and quantified using Wimasis tube analysis software (Wimasis GmbH).

Endothelial sprouting assay

Endothelial subsets of spheroids (1,000 cells per spheroid) were generated and embedded into fibrin gels. In brief, 40 EC spheroids per gel were harvested and resuspended in

460 μL of endothelial basal medium (ECGM; PromoCell), 20 μL × 10 medium-199 (Thermoscientific), and 25 μL of fibrinogen (50 mg/mL; CalBiochem). After resuspension, 5 μL of thrombin (50 U/mL; CalBiochem) was added to start polymerization of the gel. The spheroid-containing gel was rapidly transferred into prewarmed 24-well plates and allowed to polymerize for 30 min at 37°C. Thereafter, the gels were overlaid with the ECGM containing 10% FCS medium and supplemented with recombinant VEGF (25 ng/mL) and bFGF (25 ng/mL). The gels were incubated for 48 h at 37°C in 5% CO₂ at 100% humidity. For quantitative analysis of in-gel angiogenesis, the cumulative length of all capillary-like sprouts originating from the central plain of an individual spheroid was measured. Five spheroids per experimental group were analyzed. Mean values and standard deviations are shown.

FIG. 1. Characterization of V⁺ EC subsets. **(A)** Schematic representation of isolation of V⁺ endothelial subsets from hESCs after 5 days of coculture on OP9. **(B)** Phenotype and functionality of endothelial subsets studied by immunostaining, AcLDL uptake, tube formation, and sprouting. **(C)** Length of the tubes formed by each subset was measured using Wimasis SS software. **(D)** Sprout length of each subset was measured manually using the microscope. **(E)** Quantitation of the clonogenic and proliferative potential at the single-cell level in studied EC subsets. The percentage of single ECs undergoing at least 1 cell division after 14 days of culture is shown. **(F)** Number of cell progeny derived from a single EC in an individual well after 14 days of culture. Results represent the average ± SEM of three independent experiments. **P* < 0.05 by Student paired *t* test. Scale bar represents 100 μm. AcLDL, acetylated low-density lipoprotein; EC, endothelial cell; hESC, human embryonic stem cell.



Wound healing assay

V⁺ ECs isolated from H9-EGFP ESCs were cultured on fibronectin-coated plates in TGFβ inhibitor containing ECM. The confluent monolayer of cells was scratched using a pipette tip and detached cells were aspirated and rinsed with PBS. Cell migration of EGFP cells was monitored under the Nikon Eclipse Ti-E confocal microscope at 0, 12, 24, and 48 h.

Monocytic adhesion assay

The three subsets were cultured in arterial, venous, and lymphatic conditions on fibronectin-coated plates for 14 days. On day 14, cells were washed and incubated for 4 h with or without recombinant IL-1β (Peprotech). H9- GFP ES cells were differentiated to generate monocytes, as previously described [26]; 5 × 10⁶ GFP monocytes were added to each well of endothelial culture and incubated for 10 min

with gentle agitation. Unattached monocytes were removed by rinsing with medium three times before cultures were fixed in 4% PFA, followed by CD31 staining. The remaining attached monocytes were counted and normalized by the area of each individual endothelial sheet using ImageJ software (arbitrary unit).

RNA extraction and quantitative RT-PCR

RNA was extracted with the Illustra RNAspin mini RNA isolation kit (GE Healthcare) and reverse transcribed using the Advantage RT-for-PCR kit (Clontech). Quantitative RT-PCR analysis was performed for all cDNA samples using specific primers and Power SYBR Green PCR master mix (Life Technologies). PCR was performed using the Mastercycler realplex thermal cycler (Eppendorf), and expression levels were calculated by minimal cycle threshold values (Ct) normalized to GAPDH. In some cases, the gene expression was

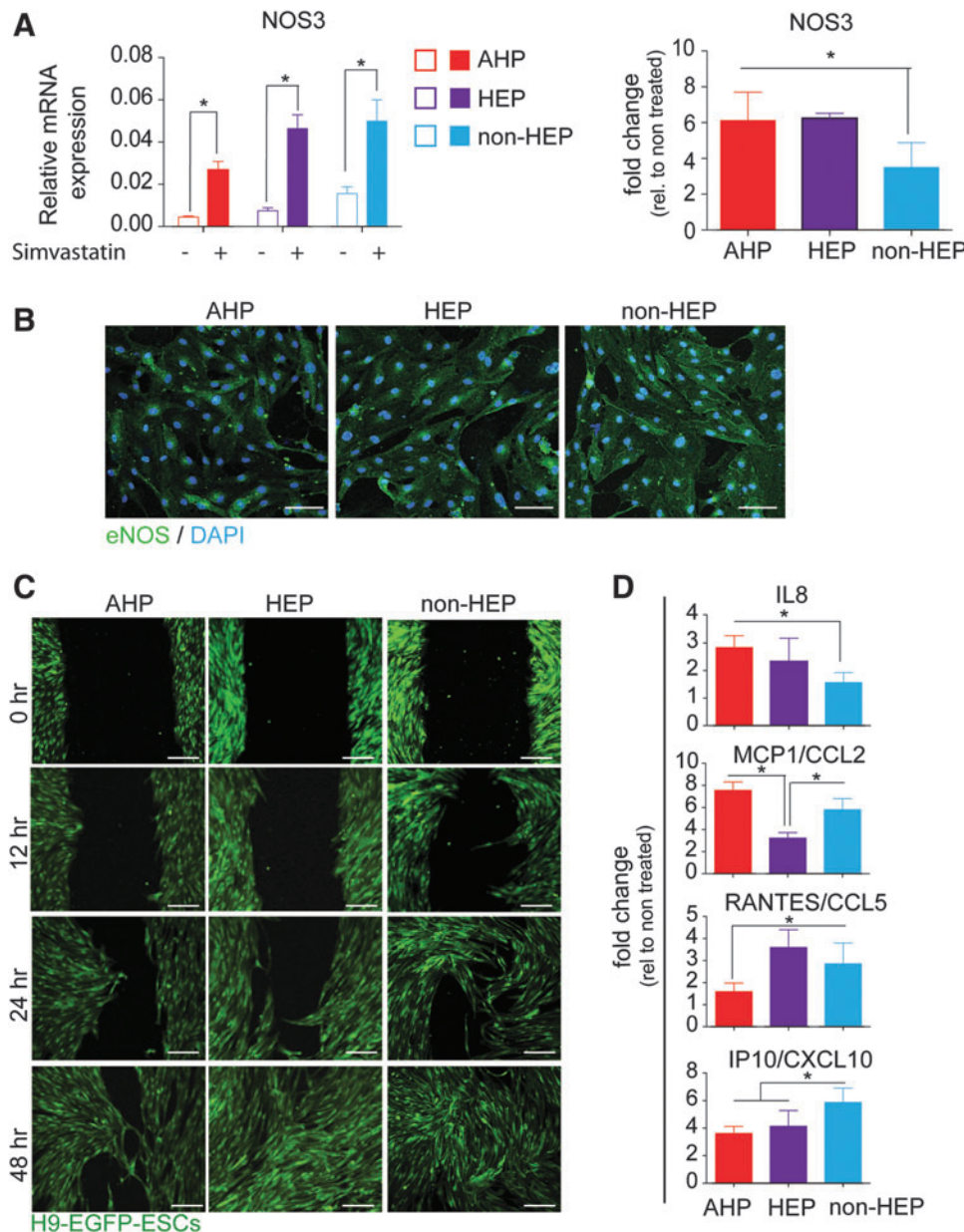


FIG. 2. Day 5 V⁺ ECs possess functional properties. **(A)** Day 5 subsets were either not treated or treated with simvastatin for 24 h, RNA was isolated, cDNA transcribed, and expression of NOS3 was studied by qRT-PCR. *Left* graph shows relative expression and *right* graph presents fold change in the expression of NOS3 in treated cells compared with the untreated. **(B)** Day 5 subsets treated with simvastatin for 24 h were immunostained for eNOS. Scale bar represents 50 μm. **(C)** Confluent monolayers of ECs derived from three V⁺ ECs generated from H9-EGFP hESCs were scratched using a pipette tip and migration of the cells was monitored for 0, 12, 24, and 48 h. Scale bar represents 100 μm. **(D)** Day 5 subsets were either not treated or treated with TNFα and INFγ for 24 h, and expression of IL8, CCL2, CCL5, and CXCL10 was studied by qRT-PCR. Results represent the average ± SEM of three independent experiments. *P < 0.05 by Student *t* test. eNOS, endothelial nitric oxide synthase.

presented as fold changes compared with the untreated samples. Primer sequences are listed in Supplementary Table S1 (Supplementary Data are available online at www.liebertpub.com/scd).

Statistical analysis

Values were analyzed for statistical significance using an unpaired Student *t*-test. Statistical significance was defined when $P < 0.05$.

Results

Characterization of functionally distinct ECs from V^+ cells

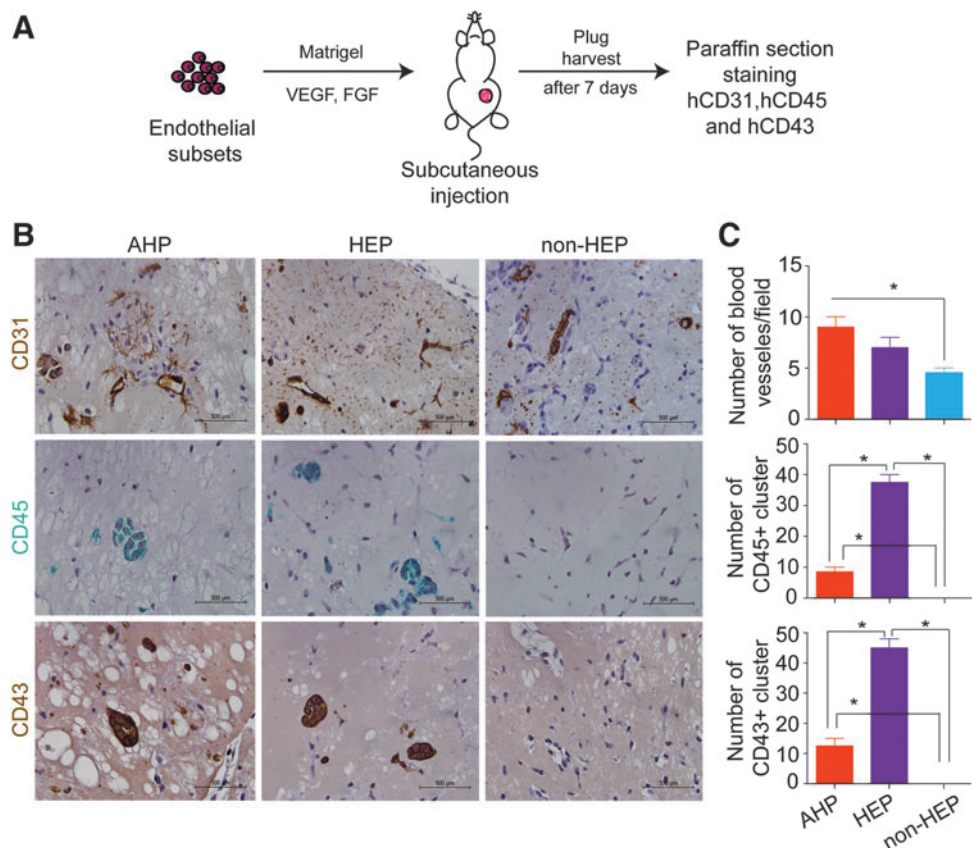
To assess endothelial properties of VE-cadherin⁺ cell subsets identified in our prior studies [17], we differentiated hESCs in the OP9 coculture system for 5 days [27,28] and isolated all three major cell subsets, as demonstrated in Fig. 1A and B. When cultured on fibronectin in standard EC culture medium, all 3-day $5 V^+$ subsets (HEPs, AHPs, and non-HEPs) formed a monolayer of adherent cells with endothelial morphology, which were capable of uptaking acetylated low-density lipoprotein (AcLDL), indicative of endothelial function (Fig. 1B). However, the studied cell subsets demonstrated some differences in Matrigel tube formation assay. The mean tube lengths (Fig. 1C) and sprouting lengths (Fig. 1D) formed by AHPs and HEPs were not different, while tubes and sprouts formed by non-HEPs were significantly shorter. To confirm the reproducibility of the obtained result, we performed similar studies in fibroblast-

derived iPSCs. Similar to hESCs, all three V^+ subsets from hiPSCs generated endothelium with the capacity to form tubes, with the highest tube length observed in AHPs (Supplementary Fig. S1A, B).

To determine the frequency of endothelial progenitors and their proliferative potential within each subset, we conducted a single-cell deposition assay using FACS (Fig. 1E). Remarkably, the percentage of single cells undergoing at least 1 cell division was higher for HEP and non-HEP ECs compared with AHPs (Fig. 1E). More than 50% of the single EC subsets that divided gave rise to small colonies or clusters ranging from 5 to 100 cells each (Fig. 1F). Approximately 20% of single ECs within HEP and non-HEP populations did form colonies containing more than 100 cells, but no colonies of more than 100 cells were observed in AHP ECs. In addition, the number of small colonies (0–5 cells) was higher in the AHP population compared with HEP and non-HEP ECs (Fig. 1F). Thus, our single-cell studies demonstrated that different subsets of ESC-derived ECs have distinct endothelial, proliferative, and clonogenic potentials in addition to differences in their ability to form blood identified in our prior studies.

Nitric oxide production is a known characteristic of ECs. To further elucidate endothelial properties of the three V^+ subsets, we studied eNOS (or NOS3) production in response to simvastatin, an HMG-CoA reductase inhibitor known to upregulate eNOS. These studies revealed the highest basal level NOS3 production in non-HEPs (Fig. 2A). Although treatment with 10 μ M of simvastatin for 24 h increased NOS3 mRNA levels in all subsets, the response to simvastatin was more pronounced in AHPs and HEPs as determined by the

FIG. 3. In vivo assessment of hESC-derived EC subsets. (A) Schematic representation of the in vivo studies. Endothelial spheroids were mixed with VEGF and FGF and injected subcutaneously into mice along with Matrigel, fibrin, and thrombin. (B) Histochemical representation of microvessels and cell aggregates formed by hESC-derived day 5 EC subsets in vivo. The paraffin sections were stained for hCD31, hCD43, and hCD45 antibodies. (C) The numbers of CD31-positive microvessels and CD43- and CD45-positive cell clusters were counted manually. Scale bar represents 500 μ m. * $P < 0.05$ by Student paired *t* test. VEGF, vascular endothelial growth factor; FGF, fibroblast growth factor.



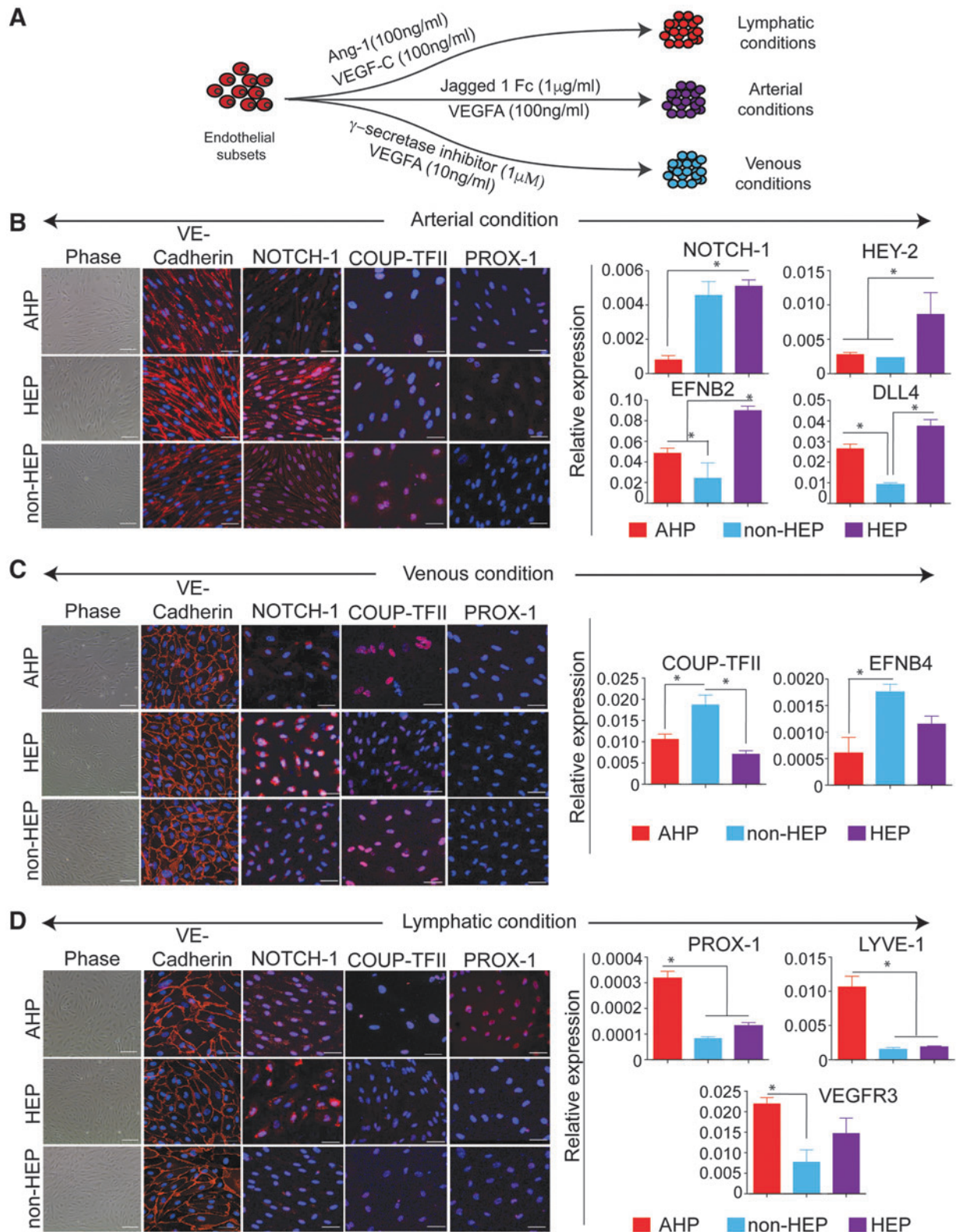
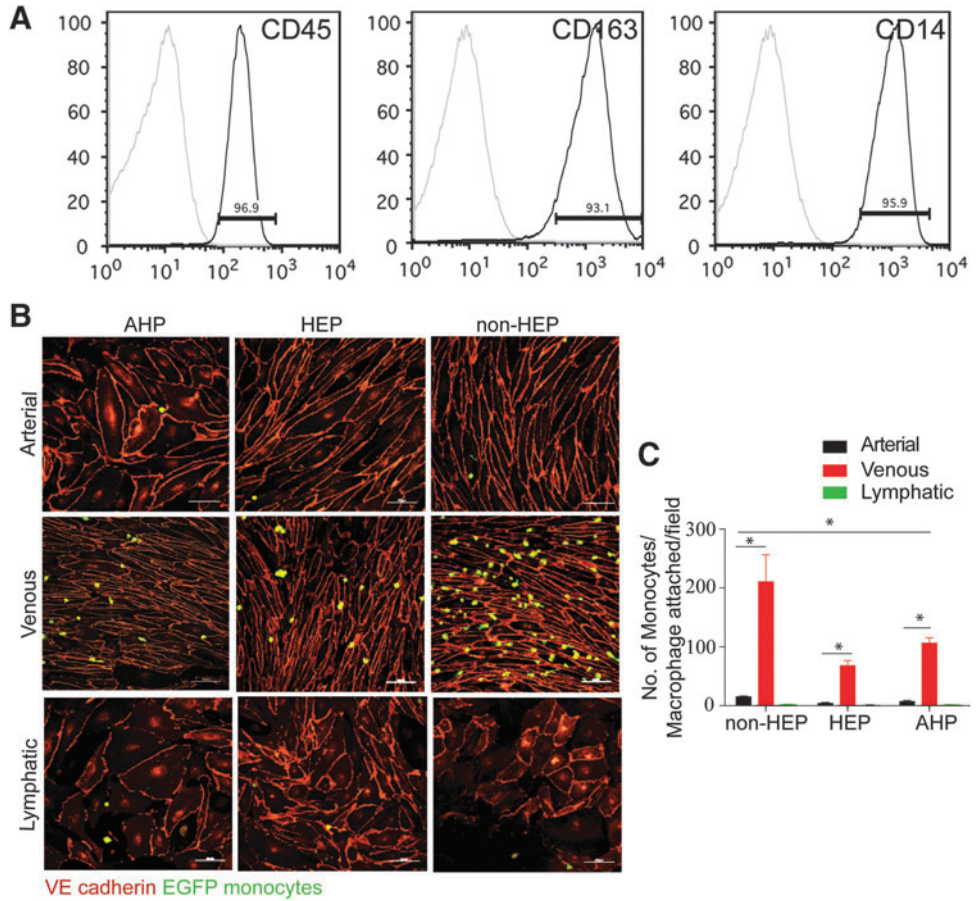


FIG. 4. V⁺ day 5 EC subsets have distinct arterial, venous, and lymphatic fates. **(A)** Schematic representation of culture conditions of the V⁺ ECs favoring arterial, venous, and lymphatic specification. **(B, C, D)** Day 5 subsets in the arterial, venous, and lymphatic conditions were immunostained for VE-cadherin, NOTCH-1, COUP-TFII, and PROX-1. In addition, arterial, venous, and lymphatic markers were analyzed by qPCR. Scale bar represents 100 µm for phase-contrast images and 50 µm for immunofluorescence images. Results represent the average ± SEM of three independent experiments. **P* < 0.05 by Student paired *t* test.

FIG. 5. Day 5 endothelial subsets have monocytic adhesiveness in response to inflammatory stimuli. **(A)** H9-GFP ESCs were differentiated in OP9 coculture for 9 days, the myeloid progenitors were expanded for 2 days and cultured in monocyte-inducing conditions for 7 days. The presence of monocytic cells was confirmed by flow cytometry. **(B)** Endothelial sheets were stimulated in the presence of IL-1 β for 4 h and GFP monocytes were allowed to adhere. An image of monocytes adhered to endothelial sheets was taken. **(C)** The number of monocytes attached to the endothelial sheets was counted. Scale bar represents 100 μ m. Results represent the average \pm SEM of three independent experiments. * $P < 0.05$ by Student paired t test.

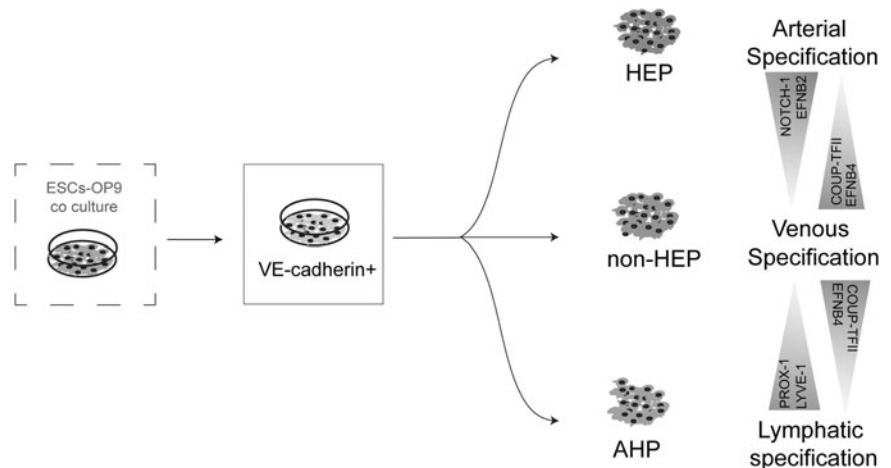


ratio of *NOS3* expression in the presence versus absence of simvastatin (Fig. 2A). *NOS3* expression following simvastatin treatment was confirmed by immunofluorescence (Fig. 2B).

We also assessed if the three EC subsets performed differently in a wound healing assay using H9-EGFP cells for better visualization of cell migration in the scratched area. Of the three subsets, the HEP and non-HEP subsets were able to fill up the scratched area in 48 h (Fig. 2C), while AHPs demonstrated delayed migration and healing of the scratched area. Another essential feature of ECs is response to inflam-

matory stimuli. To study this property, we treated the three subsets with TNF α and INF γ for 24 h and analyzed the mRNA expression of *IL8*, *CCL2/MCP-1*, *CCL5/RANTES*, and *CXCL10/IP10* proinflammatory cytokines. These studies revealed that all three EC subsets respond to TNF α and INF γ by upregulating expression of inflammatory cytokines. However, we noted that AHPs tended to produce lower amounts of *RANTES* and *IP10* and higher amounts of *IL8* and *MCP1* mRNAs, while non-HEPs typically produced lower levels of *IL8* and higher levels of *IP10* mRNAs (Fig. 2D).

FIG. 6. Schematic summary of the arterial, venous, and lymphatic differentiation potential of V⁺ EC subsets.



Transplantation of day 5 EC subsets results in formation of microvessels

After studying the in vitro potential of day 5 EC subsets, we investigated whether these ECs have the potential to form microvessels upon transplantation into a mouse model. EC subsets as spheroids were generated using methylcellulose, suspended in Matrigel, fibrin, and thrombin along with VEGF and FGF, and injected subcutaneously into the mice (Fig. 3A). The plug was harvested after 7 days and paraffin sections were stained with hCD31, hCD43, and hCD45. The antibodies used did not cross-react with the mouse. Matrigel plugs implanted with all 3 subsets showed the presence of microvessels within the matrix, which stained positive for human CD31 antibody, indicative of their human origin (Fig. 3B). Interestingly, HEPs and AHPs also showed the presence of human CD45- and CD43-positive clusters, which were not seen in the non-HEP subset (Fig. 3B). Clusters from each subset were counted manually using the Nikon Microphot SA microscope. The HEP subset showed the highest number of clusters that stained positive with hCD45 or hCD43 antibodies (Fig. 3C). These findings are consistent with our prior studies that demonstrated the hemogenic potential of CD73⁻ EC subsets in vitro.

PSC-derived endothelial subpopulations are skewed toward distinct arterial, venous, and lymphatic fates

To determine whether different V⁺ EC subsets are able to differentiate into distinct vascular lineages, we cultured FACS-sorted cells in arterial, venous, and lymphatic culture conditions for 14 days (Fig. 4A). qPCR analysis of arterial, venous, and lymphatic marker expression of freshly sorted EC subsets revealed expression of both venous and arterial markers, although AHPs demonstrated lower levels of these markers (Supplementary Fig. S2A). However, in arterial cultures, only HEP subsets showed simultaneous upregulation of NOTCH1, HEY2, EFNB2, and DLL4 arterial markers, as determined by immunofluorescence and qPCR (Fig. 4B). In the venous condition, the non-HEP subset displayed a higher affinity toward venous lineage as seen by positive staining for COUP-TFII. Expression levels of *COUP-TFII* and *EFNB4* genes were also higher in this subset compared with the other two subsets (Fig. 4C). Of the three subsets that were cultured in lymphatic conditions, only the AHP subset showed distinct lymphatic features, as evidenced by positive PROX-1 staining and greater expression of *PROX-1*, *LYVE-1*, and

VEGFR3 lymphatic markers by qPCR (Fig. 4D). Similar results were seen using V⁺ ECs from fibroblast-derived iPSCs (Supplementary Fig. S2B).

Monocytic adhesiveness in response to inflammatory stimuli is a characteristic of the venous endothelium. We took advantage of this property to confirm that ECs with arterial or venous phenotype possessed corresponding functional properties. The arterial, venous, and lymphatic endothelial cultures were generated from three EC subsets, as described above, and incubated with IL-1 β for 4 h. Subsequently, H-9 eGFP-derived monocytes (Fig. 5A) were added to the cultures and incubated for 10 min. Unattached cells were rinsed off using PBS. As seen in Fig. 5B and C, only cells cultured in venous conditions showed distinct monocyte adhesion. Importantly, monocyte adhesion was the most pronounced in venous cultures of non-HEPs, confirming that this subset skewed toward venous differentiation.

Discussion

During development, ECs emerge de novo from the mesoderm to form a primary vascular plexus. Further specialization of the endothelium to arterial, venous, hemogenic, and lymphatic subtypes is necessary to fulfill diverse functions of the vasculature [15,16]. Knowledge about various molecular pathways involved in the specification to various endothelial lineages has become extremely important, not only in the context of development but also in understanding diseases of arteries or veins specifically [29–31].

In our previous studies, we have shown that ECs can be derived from hESCs by coculturing with an OP9 feeder layer [17]. The emerging ECs generated on day 5 of differentiation can be identified by the expression of VECadherin and CD31 and further separated into subsets based on the presence or absence of CD73 and CD43/235a expression. We also have shown that these subsets have distinct blood-forming potential.

In the present studies, we investigated whether the identified EC subsets possess distinct endothelial properties. We have found that each subset of emerging V⁺CD31⁺ ECs differs in frequency of clonogenic progenitors and their proliferative potential, wound healing capacity, eNOS, and inflammatory cytokine production. Importantly, we revealed that different V⁺CD31⁺ subsets also have different capacities to support arterial, venous, and lymphatic properties when cultured in corresponding conditions. Specification to various lineages occurs very early in development and is influenced by NOTCH signaling activation [32–34]. Several studies have

TABLE 1. PHENOTYPIC FEATURES AND CHARACTERISTICS OF SUBSETS

Cell feature	AHP	HEP	Non-HEP
Endothelial type	Lymphatic	Arterial	Venous
Clonogenic potential	Low	High	High
Tube length	Long	Long	Short
Sprout length	Long	Long	Short
NOS3 in response to simvastatin	High	High	Low
Wound healing	Slow in migration	Fills up in 48 h	Fills up in 48 h
CD43/CD45+ve clusters in vivo	+	++	-
Differentiation potential	Hematoendothelial	Hematoendothelial	Endothelial

AHP, angiogenic hematopoietic progenitor; HEP, hemogenic endothelial progenitor.

shown that expression of arterial markers such as EFNB2, DLL4, NOTCH1, and NOTCH4 has been upregulated in response to higher concentrations of VEGF, while lower concentrations led to venous identity [23,24,35,36]. In our system too, we found that high concentration of VEGF in the presence of Jagged-1 and cAMP significantly increased the expression of arterial genes. However, this effect was seen specifically in the HEP subset. Similarly, inhibiting the Notch pathway using γ -secretase inhibitor and lowering the concentration of VEGF led to a venous phenotype, predominantly in the non-HEP subset.

The lymphatic system plays a crucial role in both normal and pathological conditions of the body [37,38]. Considerable research has been accomplished that provides insights into lymphatic specification and growth [39]. Similar to blood cells emerging from the hemogenic endothelium, lymphatic endothelial cells bud from a subset of ECs in the cardinal vein. The process of lymphatic cell budding is regulated by the master regulator PROX-1 [40–42]. In our system, we found that the AHP subset in the presence of VEGF-C and Ang-1 skewed toward a lymphatic phenotype by upregulating the expression of PROX1, LYVE1, and VEGFR3. As we revealed in prior studies [17], AHP cells, in contrast to other V⁺CD31⁺ subsets, have a predominantly round morphology consistent with budding cells, which could represent blood cells or budding lymphatic endothelial progenitors. As we found in previous studies, differentiation potential of non-HEPs is restricted to ECs, while HEP and AHP cells possess at least bipotential cell properties and have the capacity to form both endothelial and blood cells. At the moment, it remains unclear whether blood and endothelial potential of these subsets could be related to the heterogeneity within each subset due to the presence of distinct hemogenic and nonhemogenic ECs or if each subset contains bipotential hematoendothelial progenitors that can undergo endothelial or hematopoietic differentiation depending on specific environmental signaling. Our studies using single-cell sorting have revealed the presence of bipotential hematoendothelial progenitors within the HEP population. However, no such progenitors were detected following NOTCH activation in single-cell cultures on OP9-DLL4. In contrast, NOTCH inhibition with DAPT increased the frequency of bipotential cells, thus suggesting the existence of bipotential hematoendothelial cells whose fate can be determined by environmental signaling.

Overall, EC subsets derived from hPSCs have distinct characteristics and have the capacity to incline to arterial, venous, or lymphatic phenotypes (Fig. 6 and Table 1). These findings suggest that strategies to enhance production and selection of a particular EC subset may aid in generating desirable EC populations with arterial, venous, or lymphatic properties. In addition, functional heterogeneity within hPSC-derived ECs should be explored for selecting optimal EC populations to be used for therapeutic angiogenesis and in vitro vascularization of engineered organs in appropriate clinical settings.

Acknowledgments

The authors thank Dr. Toru Nakano for providing OP9 cells, Mitch Probasco for cell sorting, and Mathew Raymond for editorial assistance. This work was supported by funds

from the National Institutes of Health (U01HL099773, U01HL134655, P51 RR000167) and the Charlotte Geyer Foundation.

Author Disclosure Statement

No competing financial interests exist.

References

- Aird WC. (2007). Phenotypic heterogeneity of the endothelium: I. Structure, function, and mechanisms. *Circ Res* 100:158–173.
- Aird WC. (2007). Phenotypic heterogeneity of the endothelium: II. Representative vascular beds. *Circ Res* 100:174–190.
- Nolan DJ, M Ginsberg, E Israely, B Palikuqi, MG Poulos, D James, BS Ding, W Schachterle, Y Liu, et al. (2013). Molecular signatures of tissue-specific microvascular endothelial cell heterogeneity in organ maintenance and regeneration. *Dev Cell* 26:204–219.
- Risau W. (1995). Differentiation of endothelium. *FASEB J* 9:926–933.
- Cleaver O and DA Melton. (2003). Endothelial signaling during development. *Nat Med* 9:661–668.
- Garlanda C and E Dejana. (1997). Heterogeneity of endothelial cells. Specific markers. *Arterioscler Thromb Vasc Biol* 17:1193–1202.
- Rajotte D, W Arap, M Hagedorn, E Koivunen, R Pasqualini and E Ruoslahti. (1998). Molecular heterogeneity of the vascular endothelium revealed by in vivo phage display. *J Clin Invest* 102:430–437.
- Butler JM, H Kobayashi and S Rafii. (2010). Instructive role of the vascular niche in promoting tumour growth and tissue repair by angiocrine factors. *Nat Rev Cancer* 10:138–146.
- Poulos MG, P Ramalingam, MC Gutkin, M Kleppe, M Ginsberg, MJ Crowley, O Elemento, RL Levine, S Rafii, et al. (2016). Endothelial-specific inhibition of NF-kappaB enhances functional haematopoiesis. *Nat Commun* 7:13829.
- Rafii S, JM Butler and BS Ding. (2016). Angiocrine functions of organ-specific endothelial cells. *Nature* 529:316–325.
- Rafii S and D Lyden. (2003). Therapeutic stem and progenitor cell transplantation for organ vascularization and regeneration. *Nat Med* 9:702–712.
- Rafii S, D Lyden, R Benezra, K Hattori and B Heissig. (2002). Vascular and hematopoietic stem cells: novel targets for anti-angiogenesis therapy? *Nat Rev Cancer* 2:826–835.
- Chong DC, Y Koo, K Xu, S Fu and O Cleaver. (2011). Stepwise arteriovenous fate acquisition during mammalian vasculogenesis. *Dev Dyn* 240:2153–2165.
- Moyon D, L Pardanaud, L Yuan, C Breant and A Eichmann. (2001). Plasticity of endothelial cells during arterial-venous differentiation in the avian embryo. *Development* 128:3359–3370.
- Belausssoff M, SM Farrington and MH Baron. (1998). Hematopoietic induction and respecification of A-P identity by visceral endoderm signaling in the mouse embryo. *Development* 125:5009–5018.
- Vokes SA and PA Krieg. (2002). Endoderm is required for vascular endothelial tube formation, but not for angioblast specification. *Development* 129:775–785.
- Choi KD, MA Vodyanik, PP Togarrati, K Suknuntha, A Kumar, F Samarjeet, MD Probasco, S Tian, R Stewart, JA Thomson and Slukvin, II. (2012). Identification of the hemogenic endothelial progenitor and its direct precursor in

- human pluripotent stem cell differentiation cultures. *Cell Rep* 2:553–567.
18. Yu J, MA Vodyanik, K Smuga-Otto, J Antosiewicz-Bourget, JL Frane, S Tian, J Nie, GA Jonsdottir, V Ruotti, et al. (2007). Induced pluripotent stem cell lines derived from human somatic cells. *Science* 318:1917–1920.
 19. Vodyanik MA and Slukvin, II. (2007). Hematoendothelial differentiation of human embryonic stem cells. *Curr Protoc Cell Biol Chapter 23:Unit 23* 6.
 20. Ingram DA, LE Mead, H Tanaka, V Meade, A Fenoglio, K Mortell, K Pollok, MJ Ferkowicz, D Gilley and MC Yoder. (2004). Identification of a novel hierarchy of endothelial progenitor cells using human peripheral and umbilical cord blood. *Blood* 104:2752–2760.
 21. Alajati A, AM Laib, H Weber, AM Boos, A Bartol, K Ikenberg, T Korff, H Zentgraf, C Obodozie, et al. (2008). Spheroid-based engineering of a human vasculature in mice. *Nat Methods* 5:439–445.
 22. Kumar A, SS D'Souza, OV Moskvina, H Toh, B Wang, J Zhang, S Swanson, LW Guo, JA Thomson and Slukvin, II. (2017). Specification and diversification of pericytes and smooth muscle cells from mesenchymangioblasts. *Cell Rep* 19:1902–1916.
 23. Yurugi-Kobayashi T, H Itoh, T Schroeder, A Nakano, G Narazaki, F Kita, K Yanagi, M Hiraoka-Kanie, E Inoue, et al. (2006). Adrenomedullin/cyclic AMP pathway induces Notch activation and differentiation of arterial endothelial cells from vascular progenitors. *Arterioscler Thromb Vasc Biol* 26:1977–1984.
 24. Lanner F, M Sohl and F Farnébo. (2007). Functional arterial and venous fate is determined by graded VEGF signaling and notch status during embryonic stem cell differentiation. *Arterioscler Thromb Vasc Biol* 27:487–493.
 25. Kono T, H Kubo, C Shimazu, Y Ueda, M Takahashi, K Yanagi, N Fujita, T Tsuruo, H Wada and JK Yamashita. (2006). Differentiation of lymphatic endothelial cells from embryonic stem cells on OP9 stromal cells. *Arterioscler Thromb Vasc Biol* 26:2070–2076.
 26. Choi KD, M Vodyanik and Slukvin, II. (2011). Hematopoietic differentiation and production of mature myeloid cells from human pluripotent stem cells. *Nat Protoc* 6:296–313.
 27. Vodyanik MA, JA Thomson and Slukvin, II. (2006). Leukosialin (CD43) defines hematopoietic progenitors in human embryonic stem cell differentiation cultures. *Blood* 108:2095–2105.
 28. Vodyanik MA, J Yu, X Zhang, S Tian, R Stewart, JA Thomson and Slukvin, II. (2010). A mesoderm-derived precursor for mesenchymal stem and endothelial cells. *Cell Stem Cell* 7:718–729.
 29. Harvey NL and G Oliver. (2004). Choose your fate: artery, vein or lymphatic vessel? *Curr Opin Genet Dev* 14:499–505.
 30. Shawber CJ and J Kitajewski. (2004). Notch function in the vasculature: insights from zebrafish, mouse and man. *Bioessays* 26:225–234.
 31. Geraud C, PS Koch and S Goerdts. (2014). Vascular niches: endothelial cells as tissue- and site-specific multifunctional team players in health and disease. *J Dtsch Dermatol Ges* 12:685–689.
 32. Lawson ND, N Scheer, VN Pham, CH Kim, AB Chitnis, JA Campos-Ortega and BM Weinstein. (2001). Notch signaling is required for arterial-venous differentiation during embryonic vascular development. *Development* 128:3675–3683.
 33. Lawson ND, AM Vogel and BM Weinstein. (2002). sonic hedgehog and vascular endothelial growth factor act upstream of the Notch pathway during arterial endothelial differentiation. *Dev Cell* 3:127–136.
 34. Corada M, MF Morini and E Dejana. (2014). Signaling pathways in the specification of arteries and veins. *Arterioscler Thromb Vasc Biol* 34:2372–2377.
 35. Sriram G, JY Tan, I Islam, AJ Rufaihah and T Cao. (2015). Efficient differentiation of human embryonic stem cells to arterial and venous endothelial cells under feeder- and serum-free conditions. *Stem Cell Res Ther* 6:261.
 36. Aranguren XL, A Luttun, C Clavel, C Moreno, G Abizanda, MA Barajas, B Pelacho, M Uriz, M Arana, et al. (2007). In vitro and in vivo arterial differentiation of human multipotent adult progenitor cells. *Blood* 109:2634–2642.
 37. Nicenboim J, G Malkinson, T Lupo, L Asaf, Y Sela, O Mayseless, L Gibbs-Bar, N Senderovich, T Hashimshony, et al. (2015). Lymphatic vessels arise from specialized angioblasts within a venous niche. *Nature* 522:56–61.
 38. Tan YZ, HJ Wang, MH Zhang, Z Quan, T Li and QZ He. (2014). CD34+ VEGFR-3+ progenitor cells have a potential to differentiate towards lymphatic endothelial cells. *J Cell Mol Med* 18:422–433.
 39. Yang Y and G Oliver. (2014). Development of the mammalian lymphatic vasculature. *J Clin Invest* 124:888–897.
 40. Oliver G. (2004). Lymphatic vasculature development. *Nat Rev Immunol* 4:35–45.
 41. Tammela T and K Alitalo. (2010). Lymphangiogenesis: Molecular mechanisms and future promise. *Cell* 140:460–476.
 42. Hofmann JJ and ML Iruela-Arispe. (2007). Notch signaling in blood vessels: who is talking to whom about what? *Circ Res* 100:1556–1568.

Address correspondence to:

Saritha S. D'Souza, PhD
Wisconsin National Primate Research Center
University of Wisconsin
1220 Capitol Court
Madison, WI 53715

E-mail: dsouza2@wisc.edu

Received for publication November 9, 2017

Accepted after revision March 2, 2018

Prepublished on Liebert Instant Online March 3, 2018